Monocyte Chemoattractant Protein 1–dependent Leukocytic Infiltrates Are Responsible for Autoimmune Disease in MRL-*Fas*^{lpr} Mice

By Gregory H. Tesch,* Stefanie Maifert,* Andreas Schwarting,* Barrett J. Rollins,‡ and Vicki Rubin Kelley*

*From the *Laboratory of Molecular Autoimmune Disease, Renal Division, Brigham and Women's Hospital, Boston, Massachusetts 02115; and the ‡Department of Adult Oncology, Dana-Farber Cancer Institute, Boston, Massachusetts 02115*

Summary

Infiltrating leukocytes may be responsible for autoimmune disease. We hypothesized that the chemokine monocyte chemoattractant protein (MCP)-1 recruits macrophages and T cells into tissues that, in turn, are required for autoimmune disease. Using the MRL-*Fas*^{lpr} strain with spontaneous, fatal autoimmune disease, we constructed MCP-1–deficient MRL-*Fas*^{lpr} mice. In MCP-1–intact MRL-*Fas*^{lpr} mice, macrophages and T cells accumulate at sites (kidney tubules, glomeruli, pulmonary bronchioli, lymph nodes) in proportion to MCP-1 expression. Deleting MCP-1 dramatically reduces macrophage and T cell recruitment but not proliferation, protects from kidney, lung, skin, and lymph node pathology, reduces proteinuria, and prolongs survival. Notably, serum immunoglobulin (Ig) isotypes and kidney Ig/C3 deposits are not diminished in MCP-1–deficient MRL-*Fas*^{lpr} mice, highlighting the requirement for MCP-1–dependent leukocyte recruitment to initiate autoimmune disease. However, MCP-1–deficient mice are not completely protected from leukocytic invasion. T cells surrounding vessels with meager MCP-1 expression remain. In addition, downstream effector cytokines/chemokines are decreased in MCP-1–deficient mice, perhaps reflecting a reduction of cytokine-expressing leukocytes. Thus, MCP-1 promotes MRL-*Fas*^{lpr} autoimmune disease through macrophage and T cell recruitment, amplified by increasing local cytokines/chemokines. We suggest that MCP-1 is a principal therapeutic target with which to combat autoimmune diseases.

Key words: mouse • kidney • lung • chemokine • gene disruption

Infiltrating mononuclear leukocytes may be responsible for autoimmune tissue injury (1, 2). The migration of leukocytes through vessels and beyond the vascular compartment is dependent in part on small chemoattractant proteins called chemokines. Within the chemokine family, a series of reports suggest that monocyte chemoattractant protein (MCP)-1[1] may be responsible for inflammation in tissues during autoimmune disease. This is based on (a) MCP-1 tissue expression in human systemic lupus erythematosus, rheumatoid arthritis (3–5), and experimental mouse models of lupus (NZB/W mice) and allergic encephalomyelitis (6–7); (b) MCP-1 chemoattraction for monocytes and memory T cells (8–10); and (c) MCP-1 regulation of leukocyte function via modulation of adhesion molecule expression and T cell activation and proliferation (11–14). Thus, MCP-1 may be the principal chemokine responsible for initiating autoimmune tissue damage.

Strategies that neutralize or eliminate MCP-1 are protective in induced models of inflammation (15–19). MCP-1 antibody neutralization markedly reduces infiltrating macrophages and T cells in induced models of kidney and lung injury (16–19). However, antibody-based therapies have limitations; they do not necessarily deplete the target molecule and may even initiate harmful immune reactions. Perhaps the most convincing evidence supporting the requirement for MCP-1 in inflammation is illustrated in MCP-1 gene–disrupted mice. For example, MCP-1–deficient mice mount meager responses to inflammatory or immune stimulants, as evidenced in thioglycolate-elicited peritonitis, delayed-type hypersensitivity responses, and pulmonary granulomas (20). Furthermore, using a form of rapidly progressive kidney disease responsible for tubular and glomerular injury, nephrotoxic serum nephritis (NSN), we established that MCP-1–deficient B6/129 mice are spared from tubular but not glomerular destruction (21). This structure-spe-

[1]*Abbreviations used in this paper:* gcs, glomerular cross sections; MCP, monocyte chemoattractant protein; NSN, nephrotoxic serum nephritis; PAS, periodic acid Schiffs; PCNA, proliferating cell nuclear antigen; TECs, tubular epithelial cells.

cific protection is based on the abundant expression of MCP-1 in tubular epithelial cells (TECs) and nominal expression in glomeruli. However, the rapid pace of tissue destruction in NSN has made it difficult to identify specific molecular mechanisms of disease and is not representative of most human kidney diseases.

It is unclear whether blocking MCP-1 is a beneficial therapeutic strategy for human autoimmune diseases. MCP-1 is a member of a large family of leukocyte chemokines, and several of these chemokines are coexpressed in tissues during inflammation (22). Thus, the possibility of MCP-1 as a therapeutic target is dependent upon its relative importance among the chemokines, cytokines, and other molecules that are expressed during progressive tissue destruction. The challenge remains to determine whether the genetic deletion of MCP-1 prevents disease in progressive human illnesses and to decipher the mechanism responsible for MCP-1–mediated injury.

The MRL-*Fas*^{lpr} mouse strain is particularly valuable to understanding the pathogenesis of autoimmune disease, as tissue destruction in this model is spontaneous, predictable, steadily progressive, fatal, and shares features with human systemic lupus erythematosus (23). Furthermore, the tempo of disease is sufficiently long to tease apart pathogenesis but short enough to be economically feasible for experimental studies. The phenotypic expression of autoimmune disease in MRL-*Fas*^{lpr} mice is characterized by a large tissue infiltration of mononuclear leukocytes that is responsible for lymphadenopathy, splenomegaly, and autoimmune injury in multiple tissues, including the kidney, lung, and skin (23). Kidney disease in MRL-*Fas*^{lpr} mice is fatal and complex and consists of glomerular, tubular/interstitial, and vascular components mediated by infiltrating macrophages and T cells. Furthermore, the pathogenic events in each component within the kidney are distinctive. We reason that chemokines that recruit mononuclear leukocytes into the kidney and other tissues targeted for autoimmune disease are responsible for eliciting this cascade of events culminating in fatal autoimmune disease. Therefore, we hypothesize that MCP-1 is responsible for recruiting macrophages and T cells and thereby initiating disease in the kidney and other tissues undergoing autoimmune disease in MRL-*Fas*^{lpr} mice. To test this hypothesis, we have constructed an MCP-1–deficient MRL-*Fas*^{lpr} strain, evaluated pathology (kidney, lung, skin, lymph nodes, and spleen) and survival, and determined the mechanism responsible for leukocytic accumulation within these tissues.

Materials and Methods

Mice. MRL/MpJ^{++} (MRL^{++}), MRL/MpJ-*Fas*^{lpr}/*Fas*^{lpr} (MRL-*Fas*^{lpr}), C3H/FeJ, and C57BL/6 mice were purchased from the The Jackson Laboratory. MCP-1–intact and –deficient B6/129 mice (129SV/J × C57BL/6)F_1 were constructed as described (20). Control MCP-1–intact B6/129 mice were derived from matings of mice heterozygous for the disrupted allele. All mice were maintained in a pathogen-free animal facility.

Generating MCP-1–deficient MRL-Fas^{lpr} *Mice.* MCP-1–deficient (MCP-1$^{-/-}$) MRL-*Fas*^{lpr} mice were created by a series of genetic backcrosses using the cross-backcross-intercross scheme. MRL-*Fas*^{lpr} mice were mated with MCP-1$^{-/-}$ (129/Sv × C57BL/6) mice to yield heterozygous F1 offspring. We intercrossed F1 mice and screened the progeny by PCR amplification of tail genomic DNA for the *Fas*^{lpr} mutation and MCP-1 using specific primers (21, 24). Double homozygotes (*Fas*^{lpr}/*Fas*^{lpr}MCP-1$^{-/-}$) N1F1 progeny were backcrossed to MRL-*Fas*^{lpr} mice. B1 progeny, homozygous for the *Fas*^{lpr} mutation and heterozygous for MCP-1 (MCP-1$^{+/-}$), were intercrossed, and mice homozygous for the disrupted MCP-1 gene were selected by PCR typing for continued backcrossing. After three generations of backcross–intercross matings, this breeding scheme generated a colony of MRL-*Fas*^{lpr} mice (94% MRL-*Fas*^{lpr} background) homozygous and heterozygous for the disrupted MCP-1 gene. We analyzed the third generation, as we have previously established that there are sufficient MRL-*Fas*^{lpr} background genes to result in phenotypic changes characteristic of the wild-type MRL-*Fas*^{lpr} strain (25). In addition, we compared sex-matched littermates to minimize variability. The MCP-1$^{-/-}$ MRL-*Fas*^{lpr} mice are termed MCP-1 deficient, whereas the MCP-1$^{+/+}$MCP-1$^{+/-}$ MRL-*Fas*^{lpr} mice are termed MCP-1–intact MRL-*Fas*^{lpr} mice.

Proteinuria. Urine protein levels in MCP-1–intact and –deficient MRL-*Fas*^{lpr} mice were assessed semiquantitatively by dipstick analysis (Albustix; Bayer Diagnostic Division) on a monthly basis beginning at 2 mo of age. On the day of analysis, dipstick proteinuria measurements were taken from individual mice in the morning and evening. If the measurements were inconsistent, the animal was reassessed the following day.

Lymphadenopathy, Splenomegaly, and Skin Lesions. Protruding lymph nodes (cervical, brachial, and inguinal) and skin lesions were assessed monthly beginning at 3 mo of age. Lymph node score based on palpable nodes: 0 = none; 1 = small, at one site; 2 = moderate, at two different sites; and 3 = large, at three or more different sites. Skin lesion score by gross pathology: 0 = none; 1 = small (face or ears); 2 = moderate, <2 cm (face, ears, and back); and 3 = severe, >2 cm (face, ears, and back). Splenomegaly was determined by spleen weights.

Renal Pathology. Kidneys were fixed in 10% formalin for 24 h at 4°C. Paraffin sections (4 μm) were stained with hematoxylin and periodic acid Schiffs (PAS) reagent. We evaluated glomerular pathology by assessing 50 glomerular cross sections (gcs) per kidney and scored each glomerulus on a semiquantitative scale: 0 = normal (35–40 cells/gcs); 1 = mild (glomeruli with few lesions showing slight proliferative changes, mild hypercellularity [41–50 cells/gcs], and/or minor exudation); 2 = moderate (glomeruli with moderate hypercellularity [50–60 cells/gcs], including segmental and/or diffuse proliferative changes, hyalinosis, and moderate exudate); and 3 = severe (glomeruli with segmental or global sclerosis and/or exhibiting severe hypercellularity [>60 cells/gcs], necrosis, crescent formation, and heavy exudation). Damaged tubules (percent; consisting of dilation and/or atrophy and/or necrosis) were determined in 400 randomly selected renal cortical tubules per kidney (×400). Perivascular cell accumulation was determined semiquantitatively by scoring the number of cell layers surrounding the majority of vessel walls (score: 0 = none; 1 = <5; 2 = 5–10; and 3 = >10). Scoring was evaluated using coded slides.

Lung Pathology. The lungs were inflated and fixed with 10% formalin, and paraffin sections (4 μm) were stained with hematoxylin and PAS reagent. Perivascular and peribronchiolar infiltrates were assessed semiquantitatively in >20 vessels per section and in >20 bronchioli per section (number of cell layers surrounding

the majority of vessels or bronchioli: 0 = none; 1 = 1–3; 2 = 3–6; and 3 = >6).

Antibodies. The following primary antibodies were used for immunostaining: rat anti–mouse CD4 IgG2a clone RM4-5 (PharMingen) to detect CD4 T cells; rat anti–mouse CD8a (Ly-2) IgG2a clone 53-6.7 (PharMingen) to detect CD8 T cells; rat anti–mouse CD45R/B220 IgG2a clone RA3-6B2 (PharMingen) to detect CD4/CD8 T cells; rat anti–mouse CD21/35 IgG2b clone 7G6 (PharMingen) to detect B cells; rat anti–mouse monocyte/macrophage IgG2b clone MOMA-2 (BioSource International) and rat anti–mouse macrophage IgG2b (prepared from F4/80 hybridoma supernatant; American Type Culture Collection number HB198) to detect macrophages; rabbit anti–mouse MCP-1 IgG (Serotec Ltd.) to detect MCP-1; mouse anticytokeratin peptide 18 IgG1 clone CY-90 (Sigma Chemical Co.) to detect epithelial cells; fluorescein-conjugated mouse anti-PCNA (proliferating cell nuclear antigen) IgG1 clone 19F4 (Boehringer Mannheim) to detect proliferating cells; fluorescein-conjugated goat anti–mouse IgG (Organon Teknika) to detect mouse IgG; and fluorescein-conjugated goat anti–mouse C3 (Organon Teknika) to detect mouse complement C3. The negative isotype control antibodies for immunostaining were rat IgG2a clone R35-95, rat IgG2b clone R35-38, mouse IgG1 clone MOPC-21 (PharMingen), and normal rabbit IgG (Sigma Chemical Co.). The secondary antibodies for immunostaining were biotin-conjugated rabbit anti–rat IgG and biotin-conjugated goat anti–rabbit IgG (Vector Labs.). ELISA analysis of serum Ig (total Ig, IgM, IgG1, IgG2a, IgG2b, and IgG3) was performed using isotype-specific standards, goat anti–mouse capture antibodies, and alkaline phosphatase–conjugated goat anti–mouse detection antibodies (Southern Biotechnology Associates Inc.).

Identifying Infiltrating Cells. To analyze kidney- and lung-infiltrating T cells and interstitial macrophages, cryostat tissue sections (4 μm) were fixed in ethanol at 4°C for 10 min and immunostained with CD4, CD8, B220, and F4/80 antibody as previously described (26) using the avidin-biotin-peroxidase detection system (Vector Labs.). Glomerular macrophages were identified in 4-μm acetone-fixed tissue sections using MOMA-2 antibody as previously reported (16). Cells infiltrating within and around (peri) glomeruli were assessed by counting the number of labeled cells in 20 randomly selected glomeruli per section. The cells infiltrating around tubules were enumerated in 400 randomly selected tubules per section. Macrophages and T cells within glomeruli, adjacent to glomeruli, or adjacent to cortical tubules were expressed as a cell index (mean cell number/glomeruli × glomeruli/section; mean cell number/cortical tubule × cortical tubules/section). Peribronchial and perivascular macrophages and T cells (CD4, CD8, B220) in the lungs were assessed by measuring the unit area stained/unit length of bronchiole/vessel (five per animal) with a micrometer.

Detecting MCP-1 in Tissues. To detect MCP-1, formalin-fixed sections were deparaffinized and incubated with 20% normal goat serum for 30 min. Tissue sections were incubated with MCP-1 antibody (10 μg/ml) in 1% BSA overnight at 4°C. Bound primary antibody was labeled with biotin-conjugated goat anti–rabbit IgG for 1 h and subsequently detected using the avidin-biotin-peroxidase system (Vector Labs.). We confirmed MCP-1 antibody specificity using two methods: (a) MCP-1 was not detectable in tissue sections from MCP-1–deficient mice (negative control), and (b) MCP-1 was expressed in Western blots of cell lysates from LPS-stimulated bone marrow macrophages and mesangial cells in MCP-1–intact but not MCP-1–deficient mice, as previously reported (21). Glomerular MCP-1 immunostaining was assessed by the same scoring system used to detect glomerular infiltrating cells. We analyzed MCP-1 in cortical tubules in 400 tubules per cross section. We enumerated the kidney and pulmonary vessels and bronchioli that expressed MCP-1 in each section and recorded values as the percent positive.

Serum Immunoglobulins Profile. ELISA plates were coated overnight at 4°C with 5 μg/ml goat anti–mouse Ig capture antibodies (against total Ig, IgM, IgG1, IgG2a, IgG2b, and IgG3) in 0.1 M carbonate buffer, pH 9.4. Wells were blocked for 1 h with assay diluent (2% BSA in 0.1 M borate buffer, pH 8.0). We then added Ig standards to the plates (50 μl/well), starting at 1 μg/ml and performing a series of threefold dilutions, and assessed serum samples using serial (threefold) dilutions starting at 1:100 or 1:1,000. Standards and serum samples were incubated overnight at 4°C, and bound Ig was detected with goat anti–mouse detection antibodies conjugated with alkaline phosphatase and enzymatically developed by incubating with Sigma 104 phosphatase substrate in 9.6% diethanolamine and 0.1 mM $MgCl_2$, pH 9.8 (Sigma Chemical Co.). Absorbance was measured at 405 nm.

IgG and C3 in Kidneys. To examine IgG and C3 deposits in the kidney, we incubated cryostat-sectioned tissues (4 μm) with 20% normal goat or rabbit serum (30 min), followed by fluorescein-conjugated antibodies detecting mouse IgG or mouse C3 (30 min), washing, and mounting with Vectashield (Vector Labs.). We assessed immunofluorescence staining by titrating the antibodies on serial tissue sections using twofold dilution steps (1:100–1:25,600).

Apoptotic and Proliferating Cells In Situ. Apoptotic cells were identified in tissue sections (4 μm) using the terminal deoxynucleotide transferase–mediated dUTP-biotin nick-end labeling (TUNEL) method and immunoperoxidase staining (In Situ Cell Death Detection Kit; Boehringer Mannheim). Proliferating cells were detected by PCNA immunostaining as previously described (27). Sections were counterstained with PAS reagent to determine morphology. Apoptosis in glomeruli and tubules was assessed by counting the number of TUNEL-labeled cells in 50 glomeruli per section and 500 cortical tubules per section, respectively.

PCR Detection of MCPs and Cytokines in the Kidney. Total RNA was extracted from the snap-frozen renal cortex of half a kidney using RNAzol B (Tel-Test Inc.) and reverse transcribed using oligo-dT and the Superscript II DNA preamplification kit (GIBCO BRL). The resulting reverse transcription product was the cDNA template for PCR analysis. GAPDH (glyceraldehyde-3-phosphate dehydrogenase) expression was detected as a 500-bp product resulting from PCR with specific oligonucleotide primers (antisense, 5′-CAAAGTTGTCATGGATGACC-3′; and sense, 5′-GGTGGAGGTCGGAGTCAACG-3′; reference 21). The chemokines MCP-1, MCP-3, and MCP-5 were detected as 350-, 300-, and 370-bp PCR products, respectively, using specific oligonucleotide primers (MCP-1 antisense, 5′-GCTTGAGGTGGTTGTGGAAAA-3′; MCP-1 sense, 5′-CTCACCTGCTGCTACTCATTC-3′; MCP-3 antisense, 5′-CACATTCCTACAGACAGCTC-3′; MCP-3 sense, 5′-AGCTACAGAAGGATCACCAG-3′; MCP-5 antisense, 5′-CTCCTTATCCAGTATGGTCC-3′; and MCP-5 sense, 5′-TCTCCCTCCACCATGCAGAG-3′; references 28–30). The cytokines IFN-γ and CSF-1 were detected as 500- and 245-bp PCR products using specific primers (IFN-γ sense, 5′-CACGGCACAGTCATTGAAAGCC-3′; IFN-γ antisense, 5′-CTTATTGGGACAATCTCTTCCC-3′; CSF-1 sense, 5′-CACATGATTGGGAATGGACA-3′; and CSF-1 antisense, 5′-CAGCTGTTCAGGTTATTGGA-3′; references 31 and 32). The PCR primers and conditions were chosen so that the MCP and GAPDH products were amplified with equal efficiency.

Statistics. Data was analyzed using the Kruskal-Wallis test for

comparing survival curves, the Mann-Whitney test to compare group means, and Spearmans coefficient for correlations.

Results

Increased Expression of MCP-1 in MRL-Fas^{lpr} Tissues during Autoimmune Disease. MCP-1 is upregulated in MRL-*Fas^{lpr}* kidneys, lungs, and lymph nodes during autoimmune disease. First, we detected an increase (threefold) in MCP-1 mRNA within the renal cortex of wild-type pure MRL-*Fas^{lpr}* mice as early as 2 mo of age, as compared with the C57BL/6 strain with normal kidneys. MCP-1 mRNA increased further within the renal cortex (six- to eightfold) with advancing renal injury in these MRL-*Fas^{lpr}* mice (Fig. 1). We localized MCP-1 expression to several structures within the MRL-*Fas^{lpr}* kidney and determined that the rank order of tissue expression was tubules→glomeruli→vasculature. MCP-1 in MRL-*Fas^{lpr}* kidneys (5–6 mo of age) was almost exclusively localized within the TECs. More specifically, MCP-1 was within the proximal TECs (brush border histologic identification), whereas the distal TECs (histologic identification) were only weakly positive or negative. MCP-1 expression in MRL-*Fas^{lpr}* glomeruli was determined to be predominantly in epithelial podocytes, based on the morphological positioning of MCP-1–stained cells in glomeruli after histologic counterstaining (Fig. 2 b and Fig. 3 a), whereas lesser amounts localized within the epithelial cells and macrophages within crescents (two to three cells per crescent). Finally, MCP-1 in the vasculature within endothelial and smooth muscle cells was minimal (Fig. 3 a, insert). It is noteworthy that few (1–2%) infiltrating cells in the renal interstitium express MCP-1. Thus, kidney MCP-1 expression is almost exclusively within parenchymal cells and in epithelial cells in particular, rather than infiltrating cells.

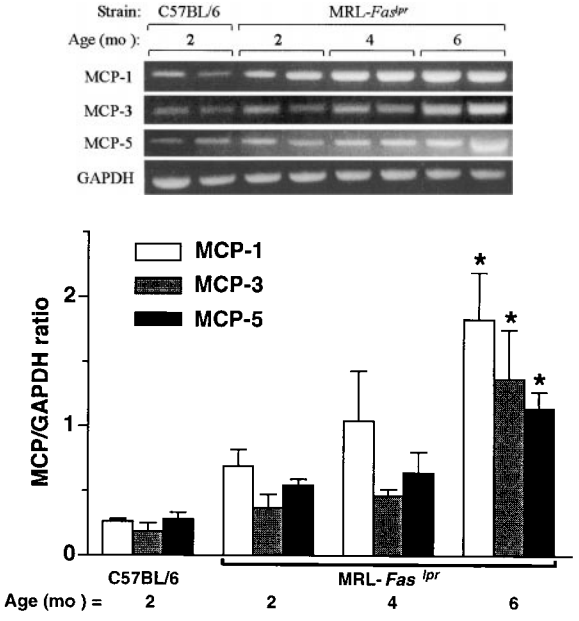

Figure 1. MCP transcripts increase with advancing disease in MRL-*Fas^{lpr}* kidneys. The renal cortex was isolated from C57BL/6 and MRL-*Fas^{lpr}* kidneys from 2 to 6 mo of age and was analyzed for MCP-1, -3, and -5 by reverse transcriptase (RT)-PCR. MCP-1, -3, and -5 are increased in MRL-*Fas^{lpr}* kidneys with progressive disease. Examples of the amplified PCR products are illustrated in the gel photos. Graph: data = mean ± SD; $n = 3$; $^*P < 0.01$ vs. MRL-*Fas^{lpr}* (2 mo).

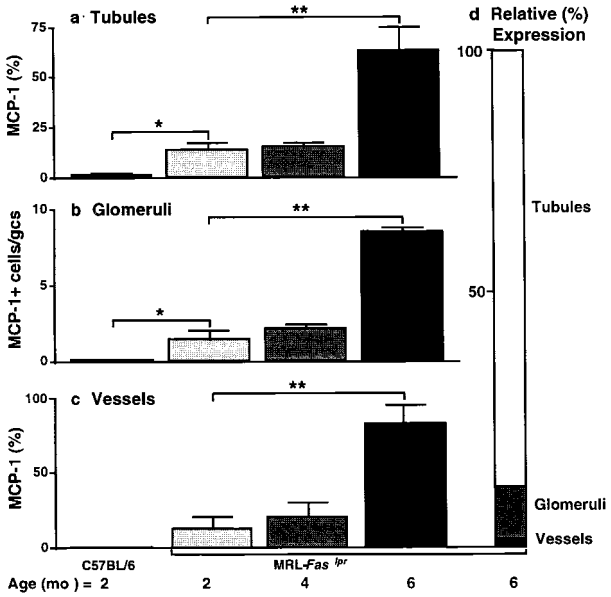

Figure 2. MCP-1 increases with advancing kidney disease in MRL-*Fas^{lpr}* mice. MCP-1 was assessed by immunostaining in (a) cortical tubules, (b) glomeruli, and (c) vessels in MRL-*Fas^{lpr}* kidneys. Data = mean ± SD; $^*P < 0.05$; $^{**}P < 0.005$. (d) The relative proportion of MRL-*Fas^{lpr}* kidney cells expressing MCP-1 was similar at 2, 4, and 6 mo of age. Few infiltrating cells in the interstitium (≤1%) express MCP-1.

MCP-1 is expressed in other tissues in MRL-*Fas^{lpr}* mice during autoimmune disease. Similar to MCP-1 in the kidney, MCP-1 in the lungs is predominantly (>90%) expressed in epithelial cells (bronchioli; Fig. 3 b) and is weakly detected within vascular endothelial and interstitial cells in MRL-*Fas^{lpr}* mice (5 mo of age). Massively enlarged lymph nodes caused by an influx of T cells are characteristic of MRL-*Fas^{lpr}* autoimmune disease (23). MCP-1 is readily detected in cells surrounding lymphatic vessels within these enlarged lymph nodes (inguinal, cervical) in MRL-*Fas^{lpr}* mice (5 mo of age; Fig. 3 c). As anticipated, MCP-1 was not detected in MCP-1–deficient MRL-*Fas^{lpr}* tissues (Fig. 3, d–f). Taken together, these data indicate that MCP-1 is mainly expressed by parenchymal cells in multiple tissues targeted for autoimmune injury in MRL-*Fas^{lpr}* mice.

MCP-1–deficient MRL-Fas^{lpr} Mice Survive Longer than MCP-1–intact MRL-Fas^{lpr} Mice and Are Protected from Proteinuria. MCP-1–deficient MRL-*Fas^{lpr}* mice have a prolonged life span as compared with MCP-1–intact MRL-*Fas^{lpr}* strains. The vast majority of MCP-1–deficient MRL-*Fas^{lpr}* mice (75%) remained alive at 300 d, as compared with a surviving minority of MCP-1–intact (MCP-$1^{+/+}$, 17% and MCP-$1^{+/-}$, 44%) MRL-*Fas^{lpr}* mice (Fig. 4 a; $P < 0.0001$). Notably, the mortality (50%) of the MCP-$1^{+/+}$ MRL-*Fas^{lpr}* strain third generation was 7 mo of age, which is similar to that of the pure wild-type MRL-*Fas^{lpr}* strain (6 mo of age)

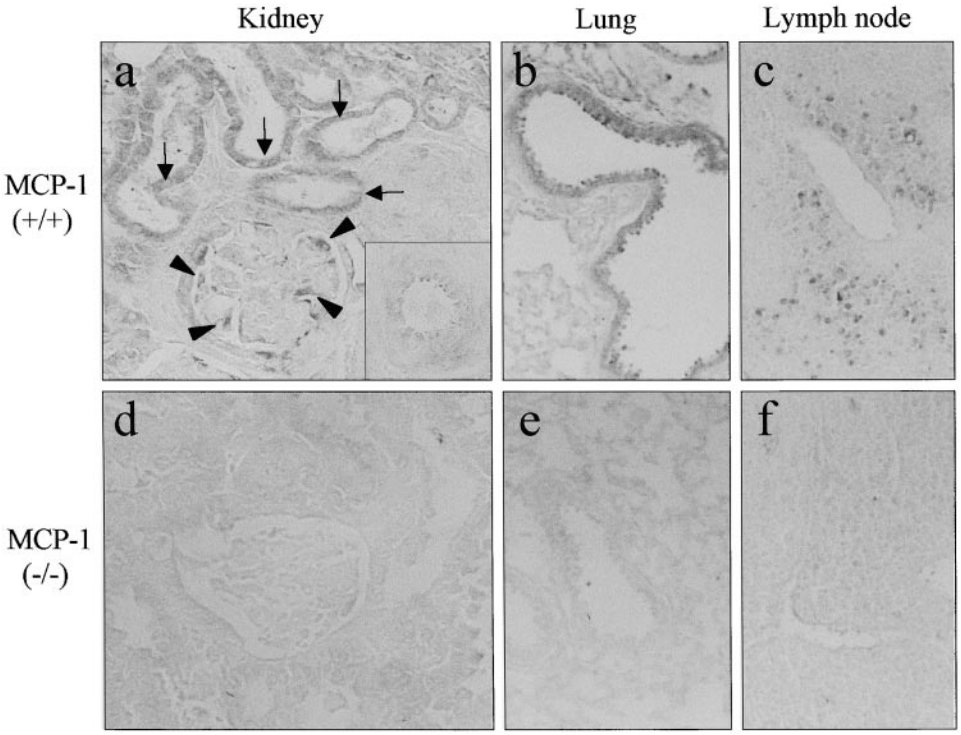

Figure 3. MCP-1 expression in MRL-*Fas*^{lpr} kidney, lung, and lymph nodes. Tissues from MCP-1–intact (a–c) and MCP-1–deficient (e and f) MRL-*Fas*^{lpr} mice at 5 mo of age were immunostained for MCP-1. MCP-1 is strongly expressed by TECs and glomerular podocytes (a) but is weak in vessels (inset) in MCP-1–intact MRL-*Fas*^{lpr} kidneys. Bronchiolar epithelial cells are the main source of MCP-1 in MCP-1–intact MRL-*Fas*^{lpr} lungs (b). A large proportion of infiltrating cells surrounding lymphatics express MCP-1 within the enlarged lymph nodes of MCP-1–intact MRL-*Fas*^{lpr} mice (c). MCP-1 is not detected in MCP-1–deficient kidney, lung, and lymph node (d–f). a and d, ×800; b, c, e, and f, ×500.

and dissimilar to that of C57BL/6J and Sv/129 strains (>20 and 16 mo of age, respectively; reference 33).

It is important to note that the spot analysis for protein in fresh individual urine specimens has several limitations, including the sample size (volume) and semiquantitative measurement. However, our confidence in making inferences from this method is enhanced by the large number of mice in each group and sequential monthly analysis. With these

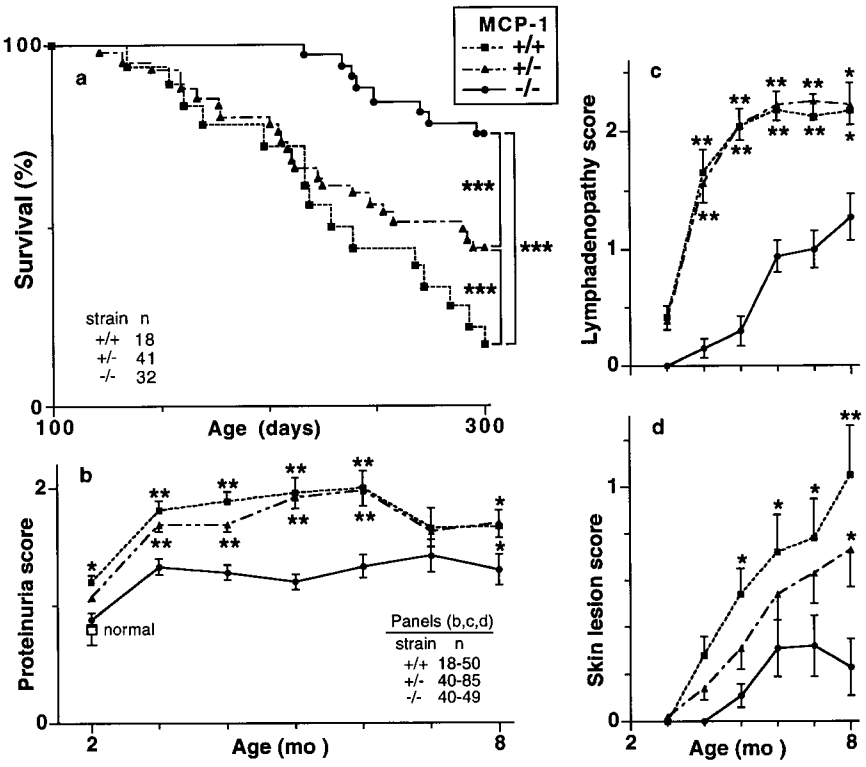

Figure 4. MCP-1–deficient MRL-*Fas*^{lpr} mice are protected from lethal autoimmune injury. (a) We evaluated survival in MCP-1–intact (+/+, +/−) and –deficient (−/−) MRL-*Fas*^{lpr} mice (<50% male and female per group). The survival of MCP-1–intact compared with –deficient MRL-*Fas*^{lpr} mice is markedly reduced ($P <$ 0.0001). In addition, MCP-1$^{+/-}$ MRL-*Fas*^{lpr} mice survive longer than the MCP-1$^{+/+}$ strain ($P < 0.0001$). (b) As the collection of small daily volumes of urine is compromised by evaporation problems, we evaluated fresh urine samples using a spot analysis. However, spot analysis in individual samples has several limitations, including small sample volume and semiquantitative measurement. With these caveats in mind, we now report that MCP-1–deficient MRL-*Fas*^{lpr} mice are protected from proteinuria (2–6 mo) in comparison to the MCP-1–intact MRL-*Fas*^{lpr} strain. The number of surviving MCP-1–intact MRL-*Fas*^{lpr} mice declines rapidly after 6 mo of age; therefore, proteinuria at these ages is limited to a subset of MCP-1–intact MRL-*Fas*^{lpr} mice, which are more resistant to disease (normal = B6/129 wild type). (c) Lymphadenopathy is reduced in MCP-1–deficient MRL-*Fas*^{lpr} mice; however, lymphadenopathy is greater in MCP-1–intact MRL-*Fas*^{lpr} females as compared with males ($P < 0.01$; females in graph). (d) Inflammatory skin lesions are reduced in MCP-1–deficient compared with –intact strains. Data = mean ± SEM; *$P < 0.05$; **$P < 0.005$; and ***$P < 0.0001$ compared with MCP-1$^{-/-}$.

caveats in mind, we now report that MCP-1–deficient versus MCP-1–intact MRL-*Fas*^{lpr} mice are protected from pathological proteinuria. From 2 to 8 mo of age, both the rate of increase and incidence of pathological proteinuria were diminished in MCP-1–deficient MRL-*Fas*^{lpr} mice (Fig. 4 b). For example, the vast majority (82%) of MCP-1–deficient MRL-*Fas*^{lpr} mice had normal, nonpathologic proteinuria (1+), whereas the majority (62%) of MCP-1–intact MRL-*Fas*^{lpr} mice were pathologically proteinuric (2–4+) at 8 mo of age. It should be noted that urinary protein in normal B6/129 wild-type mice is barely detectable (0–1+; data not shown). Thus, MCP-1–deficient MRL-*Fas*^{lpr} mice are protected from proteinuria.

Lymphadenopathy and Skin Lesions Are Reduced in MCP-1–deficient MRL-Fas^{lpr} *Mice.* We examined whether MCP-1 promotes autoimmune disease in the lymph nodes, spleen, and skin of MRL-*Fas*^{lpr} mice from 3 to 8 mo of age. The incidence and severity of lymphadenopathy and skin lesions was reduced but not totally eliminated in MCP-1–deficient as compared with MCP-1–intact MRL-*Fas*^{lpr} mice (Fig. 4, c and d). For example, although nearly every MCP-1–intact MRL-*Fas*^{lpr} mouse had palpable lymph nodes (94%), most of the MCP-1–deficient mouse lymph nodes were not palpable at 5 mo of age (69%). Similarly, the majority (84%) of MCP-1–deficient mice were spared skin lesions, whereas most (67%) of the MCP-1–intact MRL-*Fas*^{lpr} mice had gross skin pathology at 8 mo of age. On the other hand, we did not detect a difference in splenomegaly in MCP-1–deficient (234 ± 64 mg) versus MCP-1–intact MRL-*Fas*^{lpr} mice (242 ± 143 and 289 ± 174 mg MCP-1$^{+/+}$ and MCP-1$^{+/-}$, respectively; $P = 0.2$; $n = 6$ per group) at 5 mo of age.

Reduced Kidney and Lung Pathology in MCP-1–deficient MRL-Fas^{lpr} *Mice.* To determine if MCP-1 is required for kidney and lung pathology, we compared MCP-1–deficient and –intact MRL-*Fas*^{lpr} mice killed at 5 mo of age. Renal (tubular, glomerular) and pulmonary pathology was reduced in MCP-1–deficient as compared with MCP-1–intact MRL-*Fas*^{lpr} mice (Figs. 5 and 6). The reduction in tubular and glomerular pathology assessed histologically was dramatic (50–70%) in MCP-1–deficient MRL-*Fas*^{lpr} kidneys (Fig. 6, a and b; $P < 0.05$). In particular, MCP-1–deficient MRL-*Fas*^{lpr} mice had markedly diminished peritubular infiltrate, tubular atrophy, glomerular hypercellularity, glomerulosclerosis, and crescent formation. We further evaluated the level of tubular and glomerular damage by identifying apoptotic cells. The number of apoptotic cells was reduced in MCP-1–deficient versus MCP-1–intact MRL-*Fas*^{lpr} kidneys. The majority of apoptotic TECs diminished from 4.2 ± 0.3% per section in MCP-1–intact to 2.0 ± 0.6% per section in MCP-1–deficient MRL-*Fas*^{lpr} kidneys ($P < 0.05$; $n = 6$ per group). Similarly, the number of apoptotic glomerular cells was reduced in MCP-1–deficient versus MCP-1–

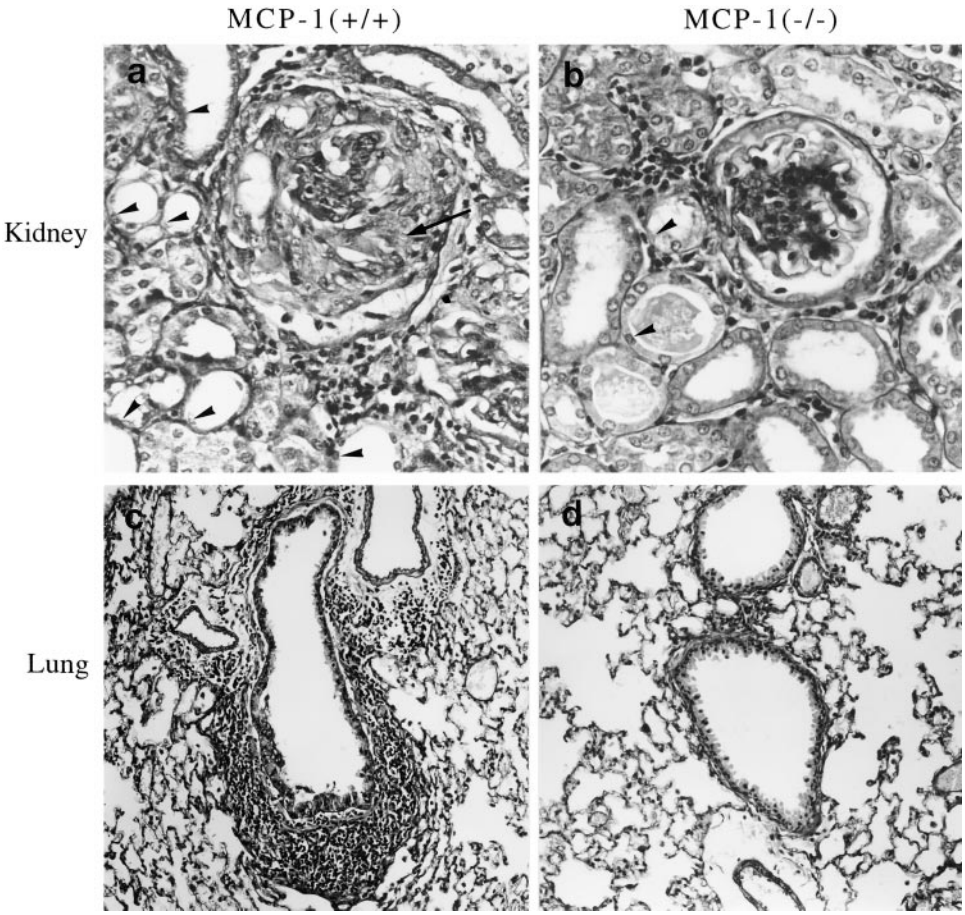

Figure 5. Kidney and lung histopathology are reduced in MCP-1–deficient MRL-*Fas*^{lpr} mice. Tubular damage (arrowheads) and glomerular crescents (arrow) are severe in MCP-1–intact MRL-*Fas*^{lpr} kidneys (a; hematoxylin and PAS) and are reduced in the MCP-1–deficient MRL-*Fas*^{lpr} strain (b) at 5 mo of age. Peribronchial and perivascular cell infiltration in MRL-*Fas*^{lpr} lungs are prominent in the MCP-1 (+/+) strain at 5 mo of age (c). By comparison, the peribronchial infiltrate is reduced in the MCP-1 (−/−) MRL-*Fas*^{lpr} strain (d). a and b, ×800; c and d, ×500.

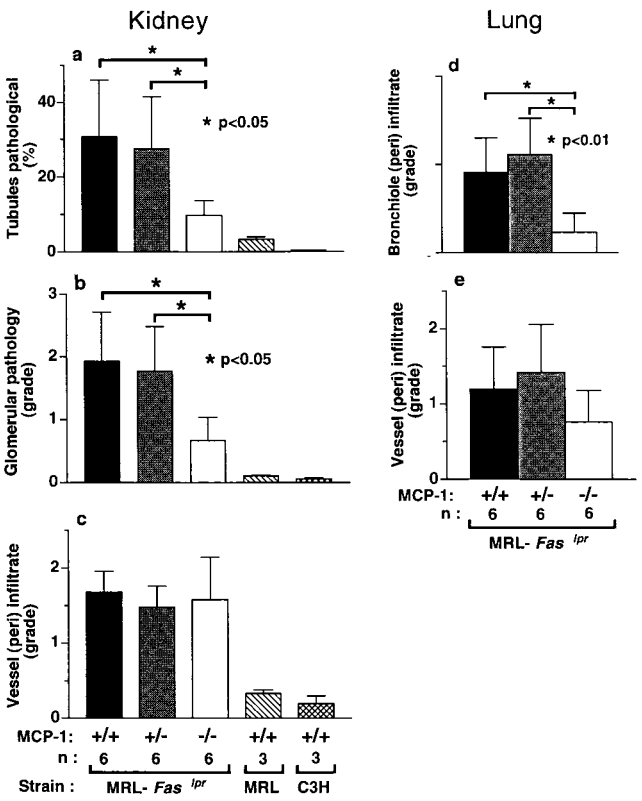

Figure 6. MCP-1–deficient MRL-*Fas*^{lpr} mice are protected from kidney and lung damage during renal disease. MCP-1 intact (+/+, +/−) and deficient (−/−) MRL-*Fas*^{lpr} kidneys were assessed for (a) tubular damage, (b) glomerular damage, and (c) perivascular cell infiltrate at 5 mo of age and compared with age-matched wild-type MRL^{++} C3H/FeJ strains. MCP-1–intact (+/+, +/−) and deficient (−/−) MRL-*Fas*^{lpr} lungs were analyzed for (d) peribronchiolar and (e) perivascular cell infiltrate at 5 mo of age. Kidney (tubular and glomerular) and lung (bronchiolar) pathology but not vasculitis was reduced in MCP-1–deficient versus MCP-1–intact MRL-*Fas*^{lpr} mice. Data = mean ± SD.

intact mice (0.11 ± 0.04 cells/gcs and 0.25 ± 0.05 cells/gcs, respectively; $P < 0.05$; $n = 6$ per group). Although there was a reduction in tubular and glomerular pathology in MCP-1–deficient MRL-*Fas*^{lpr} kidneys, it was not totally prevented (Fig. 6, a and b) in comparison to age-matched kidneys from MRL^{++} and C3H mice with normal kidneys (Fig. 6, a and b; $P < 0.005$). There was an increase in tubular and glomerular pathology in MCP-1–deficient MRL-*Fas*^{lpr} kidneys. In contrast to the protection afforded by the absence of MCP-1 in renal tubules and glomeruli of MRL-*Fas*^{lpr} mice, the perivascular infiltrates in MCP-1–deficient and –intact MRL-*Fas*^{lpr} kidneys remained similar (Fig. 6 c). Thus, MCP-1 is responsible for tubular and glomerular but not perivascular renal pathology.

Pulmonary disease was reduced in MCP-1–deficient versus MCP-1–intact MRL-*Fas*^{lpr} mice. Lung pathology in MCP-1–intact MRL-*Fas*^{lpr} mice consists of infiltrating cells predominantly surrounding bronchioles and vasculature. The numbers of cells surrounding bronchioles in MCP-1–deficient versus MCP-1–intact MRL-*Fas*^{lpr} strains was dramatically reduced (Fig. 6 d and Fig. 7, d–f; $P < 0.02$). As in the kidney, the infiltrating cells surrounding vessels were not reduced in MCP-1–deficient versus MCP-1–intact MRL-*Fas*^{lpr} lungs (Fig. 6 e; $P = 0.15$).

Less Kidney Pathology in MCP-1–deficient versus MCP-1–intact MRL-Fas^{lpr} *Mice that Do Not Survive.* We determined if the MCP-1–deficient MRL-*Fas*^{lpr} mice that died (25%; 300 d) developed renal injury that was as severe as that of the MCP-1–intact MRL-*Fas*^{lpr} mice that succumbed at considerably younger ages (83% mortality; 300 d; Fig. 4 a). The MCP-1–deficient MRL-*Fas*^{lpr} mice had less (40–50%) tubular and glomerular pathology compared with the MCP-1–intact MRL-*Fas*^{lpr} kidneys ($P < 0.05$; $n = 6$; data not shown). In addition, fewer (5/11) MCP-1–deficient MRL-*Fas*^{lpr} mice, as compared with MCP-1–intact MRL-*Fas*^{lpr} mice (12/16), died with severe proteinuria (3–4+). Thus, even in the MCP-1–deficient and MCP-1–intact MRL-*Fas*^{lpr} mice that eventually die, the extent of renal injury is less severe in the MCP-1–deficient MRL-*Fas*^{lpr} strain.

Decreased Infiltrating Cells in the Kidney (Macrophages and T Cells) and Lungs (Macrophages) in MCP-1–deficient versus MCP-1–intact MRL-Fas^{lpr} *Mice.* There was a reduction in the number of macrophages and T cells (CD4 and CD8 but not B220) in MCP-1–deficient versus MCP-1–intact MRL-*Fas*^{lpr} kidneys. The majority of macrophages and T cells localized in the interstitium adjacent to tubules and glomeruli, whereas fewer were identified within glomeruli. We noted the largest (50–72%) decline in macrophages and T cells in the MCP-1–deficient MRL-*Fas*^{lpr} strain surrounding tubules ($P < 0.01$; Fig. 7, a–c), a reduction that correlated with the extent of tubular injury ($r \geq 0.80$; $P < 0.005$). Periglomerular macrophages and CD4 but not CD8 T cells were also diminished (45–53%, $P < 0.05$) in MCP-1–deficient MRL-*Fas*^{lpr} mice (Fig. 7 a). Although intraglomerular macrophages were reduced (34%) in MCP-1–deficient MRL-*Fas*^{lpr} kidneys ($P < 0.005$; Fig. 7 a), the numbers of intraglomerular T cells (CD4, CD8, B220) were not diminished ($P = 0.2$). The reduction in glomerular macrophages correlated with diminished glomerular morphologic damage (intraglomerular, $r = 0.78$; periglomerular, $r = 0.77$; $P < 0.005$). The absence of MCP-1 in MRL-*Fas*^{lpr} lungs reduced the number of infiltrating macrophages surrounding bronchioli but not surrounding vessels (Fig. 7, d–f). In contrast to the reduction in the number of kidney-infiltrating T cells in MCP-1–deficient versus –intact MRL-*Fas*^{lpr} mice, the number of T cells (CD4, CD8, B220) in the lungs was not reduced ($P = 0.2$; Fig. 7 d).

A Reduction in Macrophages and T Cells in MCP-1–deficient Kidneys and Lungs Did Not Result from Decreased Local Proliferation. We determined if the decreased accumulation of macrophages and T cells in MCP-1–deficient MRL-*Fas*^{lpr} kidneys and lungs at 5 mo of age was a result of a decline in local proliferation using in situ detection of PCNA. First, few of the cells surrounding tubules (<1%), glomeruli (<1%), and bronchioli (<10%) were proliferating in the MCP-1–intact MRL-*Fas*^{lpr} strain. The number of PCNA^{+} cells was not reduced in the MCP-1–deficient MRL-*Fas*^{lpr} strain ($P = 0.2$; $n = 6$). Second, there were substantially more proliferating cells surrounding vessels (>20%) com-

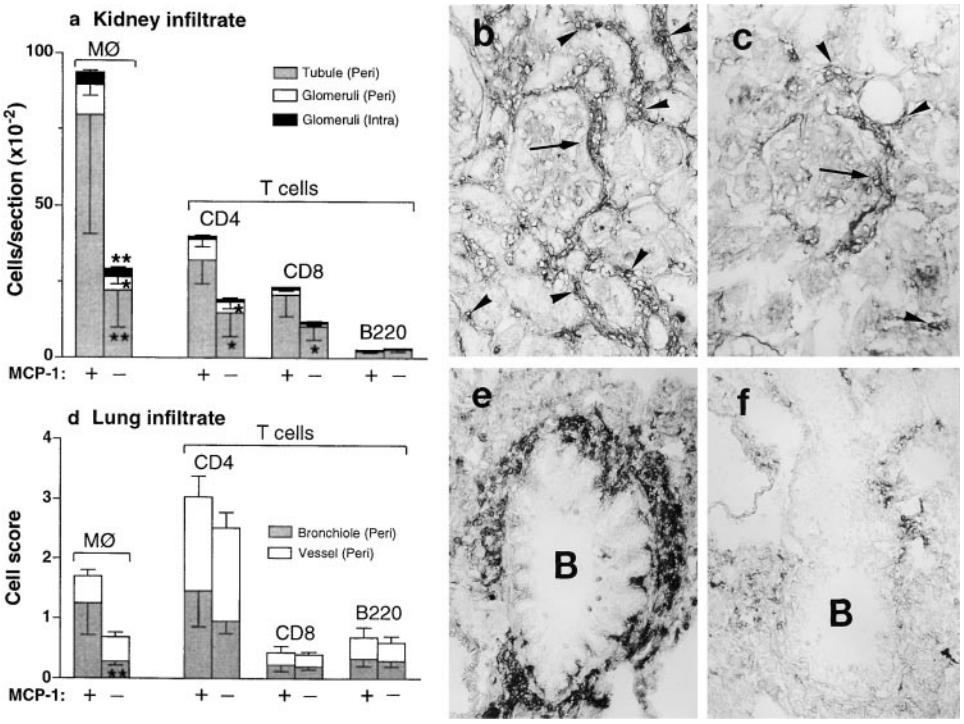

Figure 7. Kidney- and lung-infiltrating leukocytes are reduced in MCP-1–deficient MRL-*Fas*^{lpr} mice. Infiltrating leukocytes were assessed in the kidney (a–c) and lung (d–f) by immunostaining. Macrophage (MØ) accumulation adjacent to kidney parenchymal cells (peritubular, periglomerular, intraglomerular) in MCP-1–intact MRL-*Fas*^{lpr} mice (b) is markedly reduced in MCP-1–deficient MRL-*Fas*^{lpr} mice (c). Similarly, the notable macrophage accumulation adjacent to parenchymal cells in the lung (peribronchiolar) in MCP-1–intact MRL-*Fas*^{lpr} mice (e) is dramatically less in MCP-1–deficient MRL-*Fas*^{lpr} mice (f). Furthermore, T cells, including CD4 and CD8 T cells, are reduced in the peritubular area, whereas CD4 T cells accumulate less surrounding glomeruli in MCP-1–deficient versus MCP-1–intact MRL-*Fas*^{lpr} strains (a). In contrast, perivascular macrophages and T cells are not different in the MCP-1–intact and –deficient MRL-*Fas*^{lpr} lungs (d) and kidneys (not shown). Data = mean ± SD; $n = 6$; $^{*}P < 0.05$ and $^{**}P < 0.01$ compared with MCP-1$^{+/+}$. F4/80 immunostaining: b and c, ×500; e and f, ×330.

pared with proliferating cells surrounding glomeruli, tubules, and bronchioles in MCP-1–intact MRL-*Fas*^{lpr} kidneys and lungs ($P < 0.002$), and this number did not decrease in the MCP-1–deficient MRL-*Fas*^{lpr} strain ($P = 0.1$; $n = 6$ per group). Of course, it must be appreciated that the proliferation measurements in tissue sections are a reflection of the level of cell division at the time these tissues were removed. Thus, the reduction in kidney- and lung-infiltrating cells in MCP-1–deficient MRL-*Fas*^{lpr} mice does not appear to result from decreased local proliferation.

CCR2 Ligand Expression in MCP-1–deficient MRL-Fas^{lpr} *Kidneys Is Decreased.* MCPs 1–5 are ligands for the MCP-1 receptor (CCR2; reference 22). To examine whether CCR2 ligands other than MCP-1 are upregulated after renal injury, we examined MCP-3 and MCP-5 in MRL-*Fas*^{lpr} kidneys. Renal cortical transcripts of MCP-3 and MCP-5 in MRL-*Fas*^{lpr} as compared with C57BL/6 mice were increased (twofold) in advance of overt renal pathology (2 mo of age) and rose further (fourfold) as renal pathology advanced (6 mo of age; Fig. 1). We probed for MCP expression in MCP-1–deficient MRL-*Fas*^{lpr} kidneys. As anticipated, MCP-1 transcripts were not detected in the MCP-1–deficient MRL-*Fas*^{lpr} renal cortex. On the other hand, MCP-3 and MCP-5 transcripts were detected in MCP-1–deficient MRL-*Fas*^{lpr} mice (Fig. 8). However, amounts of MCP-3 and MCP-5 transcripts were 50% lower in MCP-1–deficient versus MCP-1–intact MRL-*Fas*^{lpr} kidneys ($P < 0.005$; Fig. 8). Thus, MRL-*Fas*^{lpr} mice lacking MCP-1 have reduced intrarenal productions of ligands (MCP-3, MCP-5) that bind to CCR2.

Reduced CSF-1 and IFN-γ Transcripts in MCP-1–deficient MRL-Fas^{lpr} *Kidneys.* We previously established that CSF-1 and IFN-γ transcripts that are upregulated with advancing renal injury in MRL-*Fas*^{lpr} mice are required for autoimmune kidney disease (25, 34, 35). In MCP-1–deficient MRL-*Fas*^{lpr} kidneys, CSF-1 and IFN-γ transcripts were reduced as compared with the MCP-1 intact MRL-*Fas*^{lpr} strain (Fig.

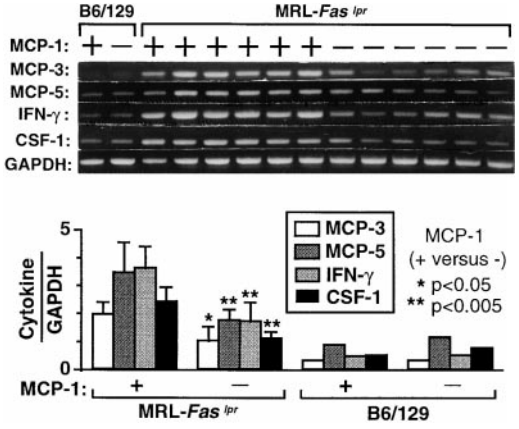

Figure 8. MCP-1 deficiency reduces CSF-1, IFN-γ, and other CCR2 ligands in MRL-*Fas*^{lpr} kidneys. Transcript levels of CSF-1, IFN-γ, MCP-3, and MCP-5 were assessed in comparison to GAPDH in MCP-1–intact and –deficient MRL-*Fas*^{lpr} and B6/129 mouse renal cortices at 5 mo of age by RT-PCR. CSF-1, IFN-γ, MCP-3, and MCP-5 transcripts were reduced in MCP-1–deficient versus MCP-1–intact MRL-*Fas*^{lpr} mice. Data = mean ± SD; $n = 6$; P values compared with MCP-1–intact MRL-*Fas*^{lpr} mice.

8). In contrast, CSF-1 and IFN-γ transcripts in MCP-1–deficient and –intact B6/129 mice with normal kidneys were barely detectable (Fig. 8).

Serum- and Kidney-deposited Igs Are Not Reduced in MCP-1–deficient MRL-Fas^{lpr} Mice. To determine if MCP-1 alters the antibody isotype profile in MRL-*Fas^{lpr}* autoimmune disease, we evaluated serum levels of IgGs (total Ig, IgM, IgG1, IgG2a, IgG2b, IgG3) in MCP-1–deficient and –intact MRL-*Fas^{lpr}* mice. We did not detect differences in serum IgGs (amount and isotype) in MCP-1–deficient and –intact MRL-*Fas^{lpr}* strains (Fig. 9 a). In addition, we did not detect an alteration in the amount and distribution of Igs within MCP-1–deficient and –intact MRL-*Fas^{lpr}* kidneys (Fig. 9 b). Similarly, complement (C3) deposition was not reduced in MCP-1–deficient as compared with MCP-1–intact MRL-*Fas^{lpr}* glomeruli (data not shown). Thus, MCP-1 does not regulate circulating or kidney-depositing IgGs in MRL-*Fas^{lpr}* mice.

Discussion

In this report, we tested the hypothesis that a specific chemokine, MCP-1, is required for autoimmune tissue injury in MRL-*Fas^{lpr}* mice. We now report that MRL-*Fas^{lpr}* mice genetically deficient in MCP-1 are partially protected from autoimmune disease, including injury to the kidney, lung, and skin and lymphadenopathy, resulting in a prolonged life span. Protection against tissue injury in MCP-1–deficient MRL-*Fas^{lpr}* mice results from a reduced infiltration of leukocytes (macrophages and T cells) toward parenchymal cells that no longer express MCP-1 and a diminution in cytokines known to promote tissue injury. Furthermore, we determined that the accumulation of these cells is a result of recruitment, but not proliferation, toward the parenchymal cells in proportion to MCP-1 expression. Thus, MCP-1 is responsible for recruiting macrophages and T cells into multiple tissues, including the kidney, lung, and lymph nodes, in MRL-*Fas^{lpr}* mice, which in turn results in autoimmune tissue destruction.

During inflammation, multiple parenchymal and leukocyte cell types express MCP-1 (36). Our challenge was to identify the cell types and locations expressing MCP-1 and determine the impact of cells producing MCP-1 on disease progression in MRL-*Fas^{lpr}* mice. We now report that MCP-1 is primarily expressed by parenchymal cells, and not infiltrating cells, in MRL-*Fas^{lpr}* mice, beginning before and then increasing during autoimmune disease. We determined that parenchymal epithelial cells express far more MCP-1 than other parenchymal cell types (endothelial cells, smooth muscle cells, and mesangial cells). Furthermore, we established that the accumulation of macrophages and T cells was directly proportional to MCP-1 expression by these parenchymal cells. This is consistent with our previous findings in a rapid, induced form of kidney damage, NSN, consisting of glomerular and tubular pathology (21). In NSN, we noted that MCP-1, abundantly expressed in TECs and barely detected in glomeruli, was responsible for tubular but not glomerular injury. We established that macrophages were recruited toward tubules expressing MCP-1 and after activation released molecules that induced TEC apoptosis (21). By comparison, the importance of MCP-1 in progressive autoimmune disease in MRL-*Fas^{lpr}* mice is broader than in NSN. First, MCP-1 is responsible for the accumulation of not only macrophages but also T cells within the kidney (tubules and glomeruli) and other tissues (lungs and lymph nodes) during autoimmune disease in MRL-*Fas^{lpr}* mice. For example, massively enlarged lymph nodes, composed of T cells, are characteristic of MCP-1–intact MRL-*Fas^{lpr}* mice (37). The most convincing evidence for MCP-1 fostering T cell accumulation is highlighted by the substantial decrease in the incidence of lymphadenopathy and lymph node size (>50% reduced at 8 mo of age) in MCP-1–deficient MRL-*Fas^{lpr}* mice. However, the numbers of T cells in the MCP-1–deficient MRL-*Fas^{lpr}* lymph nodes are not reduced to normal levels. In addition, MCP-1 is not required for splenomegaly in MRL-*Fas^{lpr}* spleens, as MCP-1–intact and MCP-1–deficient MRL-*Fas^{lpr}* spleens were similar. Thus, MCP-1 is responsible in part for lymphadenopathy, but other molecules, perhaps chemokines, are required for splenomegaly in the MRL-*Fas^{lpr}* strain. Other candidates that are likely to be involved in splenomegaly include the β-chemokines macrophage inflammatory protein (MIP)-1α and MIP-1β, reported to foster T cell trafficking (CD4, CD8) into lymph nodes after induced hypersensitivity (38). In addition, we suggest that the broader impact of MCP-1 on kidney injury in the MRL-*Fas^{lpr}* mouse versus NSN is related to the progressive accumulation of MCP-1–dependent leukocytes over a longer period of disease manifestation in the MRL-*Fas^{lpr}* kidney and other tissues. Furthermore, comparison of MCP-1 immunostaining and mRNA levels in the two models indicates that tubules and glomeruli in MCP-1–intact MRL-*Fas^{lpr}* mice (5–6 mo) express higher amounts of MCP-1 than in NSN (7 d). Disease in NSN is mostly limited to the kidney, whereas MRL-*Fas^{lpr}* mice have multiple tissues targeted for destruction, each expressing MCP-1. Thus, by gene target–deleting MCP-1 in MRL-*Fas^{lpr}* mice, we determined that MCP-1 is responsible for recruiting macrophages and T cells to numerous tissues, each undergoing autoimmune disease.

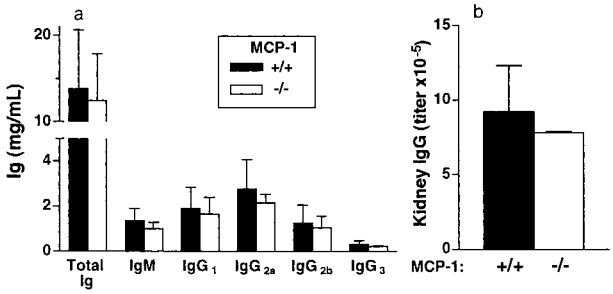

Figure 9. (a) MCP-1 deficiency does not reduce serum Ig isotype levels in MRL-*Fas^{lpr}* mice. Serum from MCP-1–intact and –deficient MRL-*Fas^{lpr}* mice at 5 mo of age was analyzed for Igs by ELISA. (b) MCP-1–deficient MRL-*Fas^{lpr}* mice (5 mo of age) have equivalent amounts of IgG and C3 (not shown) in the kidney despite a reduction in loss of renal function, glomerular and tubular injury, and enhanced survival as compared with the MCP-1–intact strain. Data = mean ± SD; $n = 6$.

The accumulation of macrophages and T cells surrounding parenchymal tissue in MRL-*Fas*^{lpr} mice results from recruitment and/or proliferation of these leukocytes (26, 27, 34, 35, 39). As MCP-1 induces IL-2 production by T cells (14), it is possible that MCP-1 promotes T cell proliferation in the kidney, lung, and lymph nodes. However, as few infiltrating cells are proliferating (PCNA$^+$) at sites of MCP-1 expression within the kidney, lung, and enlarged lymph nodes in MRL-*Fas*^{lpr} mice, we conclude that the primary action of MCP-1 is to recruit macrophages and T cells into tissues and thereby promote autoimmune disease.

To further support the concept that MCP-1 initiates kidney injury via recruitment and not other immune events, we investigated whether MCP-1 caused an Ig isotype switch and alteration in Ig deposition in the kidney. Elevated Ig levels in MRL-*Fas*^{lpr} mice are dependent on T cell (40) and B cell (41, 42) events that are independent of MCP-1 in MRL-*Fas*^{lpr} mice. In addition, isotypes such as IgG3 compromise glomerular function (43). We did not detect any difference in the serum Ig isotypes nor in the amount or location of Igs in the kidney. It is interesting to note that despite the similarly high levels of serum and glomerular Igs, the glomeruli are better preserved functionally (loss of protein) and structurally in MCP-1–deficient versus MCP-1–intact MRL-*Fas*^{lpr} mice. This suggests that, even when the Igs are deposited within the kidney, MCP-1 is required to attract leukocytes into the kidney to initiate glomerular and tubular/interstitial renal disease in MRL-*Fas*^{lpr} mice.

Protection from injury in MCP-1–deficient MRL-*Fas*^{lpr} kidneys is associated with reduced number of transcripts of the nephritogenic cytokines (IFN-γ and CSF-1) and other chemokines in addition to MCP-1 that bind to the CCR2 receptor (MCP-3 and MCP-5). This could be either directly or indirectly related to the MCP-1 deletion in MRL-*Fas*^{lpr} mice. For example, MCP-1 immunomodulation of CD4 cells is related to the release of IFN-γ (14). We suggest that after MCP-1–dependent recruitment of leukocytes into the kidney, a cascade of events triggers the production of IFN-γ, CSF-1, MCP-3, and MCP-5, which each contribute to autoimmune kidney damage. For example, we have previously established that CSF-1, a macrophage growth factor, is responsible for promoting macrophage- and T cell–initiated kidney injury (35), whereas IFN-γ, with more complex actions, either thwarts (27) or fosters (25, 44) injury depending on when it is expressed during disease. In addition, MCP-3 and MCP-5 may be responsible for the migration of leukocytes into the kidney (45). We therefore speculate that the increase in MCP-1 is a proximal stimulus responsible for recruiting macrophages and T cells, which in turn are responsible for triggering the production of cytokines and other chemokines that lead to tissue injury.

Although MCP-1 depletion dampens injury in multiple tissues during autoimmune attack, these tissues are not totally protected. The kidneys, lungs, spleen, lymph nodes, and skin do not remain normal. The renal tubule/interstitium, glomeruli, lungs, and lymph nodes in MCP-1–deficient MRL-*Fas*^{lpr} mice are still invaded by leukocytes, although in far lower numbers than in MCP-1–intact MRL-*Fas*^{lpr} mice. Additionally, the limited number of MCP-1–deficient MRL-*Fas*^{lpr} mice that do not survive kidney glomerular and tubular disease and proteinuria is far lower than younger MCP-1–intact MRL-*Fas*^{lpr} mice that succumb. In contrast, vascular disease is not prevented in MCP-1–deficient kidneys and lungs. The accumulation of leukocytes around vessels, almost exclusively T cells, is just as abundant in MCP-1–deficient versus –intact MRL-*Fas*^{lpr} kidneys and lungs. There are several possible explanations for this finding. Other chemokines may be responsible for recruiting these infiltrating leukocytes. For example, MCP-1 is weakly expressed in the vascular wall and perivascular leukocytes, whereas RANTES (regulated upon activation, normal T cell expressed and secreted) is abundant in both areas (data not shown). In addition, many perivascular leukocytes in the kidney and lung are proliferating (PCNA$^+$) and, therefore, perivascular leukocytes may accumulate because of local proliferation. It is worth noting that perivasculitis in the kidney contributes to mortality in wild-type MRL-*Fas*^{lpr} mice (45, 46) and, therefore, may be at least partially compromising in several tissues in MCP-1–deficient MRL-*Fas*^{lpr} mice. Finally, as the accumulation of leukocytes in the renal interstitium is focal in both MCP-1–intact and –deficient MRL-*Fas*^{lpr} mice, we suggest that molecules responsible for adhesion, cell activation, proliferation, and death, including integrins, selectins, and cytokines, may contribute to this process. Furthermore, we cannot rule out the possibility that other chemokines, in addition to MCP-1, enhance leukocytic recruitment. Thus, to achieve more complete protection from autoimmune disease in the MRL-*Fas*^{lpr} strain, we will have to identify additional therapeutic targets.

In conclusion, we suggest that MCP-1 is a therapeutic target to combat autoimmune/inflammatory diseases triggered by tissue leukocytic invasion. Our data further suggest that eliminating MCP-1 expression does not confer total protection. It is thus critical to identify the other therapeutic targets responsible for leukocyte invasion and expansion to confer total protection.

We wish to thank Dr. Hyung-Jin Yoon for assisting with the construction of the MCP-1–deficient MRL-*Fas*^{lpr} strain.

This work was supported in part by National Institutes of Health grants DK-36149 and DK 52369 (to V.R. Kelley) and a research fellowship from the National Kidney Foundation (to G.H. Tesch).

Address correspondence to Vicki Rubin Kelley, Harvard Institutes of Medicine, 77 Ave. Louis Pasteur, Boston, MA 02115. Phone: 617-525-5915; Fax: 617-525-5830; E-mail: vkelley@rics.bwh.harvard.edu

Submitted: 20 April 1999 Revised: 27 September 1999 Accepted: 5 October 1999

References

1. Koh, D.R., A. Ho, A. Rahemtulla, W.P. Fung-Leung, H. Griesser, and T.W. Mak. 1995. Murine lupus in MRL/lpr mice lacking CD4 or CD8 T cells. *Eur. J. Immunol.* 25:2558–2562.
2. Tran, E.H., K. Hoekstra, N. van Rooijen, C.D. Dijkstra, and T. Owens. 1998. Immune invasion of the central nervous system parenchyma and experimental allergic encephalomyelitis, but not leukocyte extravasation from blood, are prevented in macrophage-depleted mice. *J. Immunol.* 161:3767–3775.
3. Rovin, B.H., M. Rumancik, L. Tan, and J. Dickerson. 1994. Glomerular expression of monocyte chemoattractant protein-1 in experimental and human glomerulonephritis. *Lab. Invest.* 71:536–542.
4. Wada, T., H. Yokoyama, S. Su, N. Mukaida, M. Iwano, K. Dohi, Y. Takahashi, T. Sasaki, K. Furuichi, C. Segawa, et al. 1996. Monitoring urinary levels of monocyte chemotactic and activating factor reflects disease activity of lupus nephritis. *Kidney Int.* 49:761–767.
5. Harigai, M., M. Hara, T. Yoshimura, E.J. Leonard, K. Inoue, and S. Kashiwazaki. 1993. Monocyte chemoattractant protein-1 (MCP-1) in inflammatory joint diseases and its involvement in the cytokine network of rheumatoid synovium. *Clin. Immunol. Immunopathol.* 69:83–91.
6. Zoja, C., X.H. Liu, R. Donadelli, M. Abbate, D. Testa, D. Corna, G. Taraboletti, A. Vecchi, Q.G. Dong, B.J. Rollins, et al. 1997. Renal expression of monocyte chemoattractant protein-1 in lupus autoimmune mice. *J. Am. Soc. Nephrol.* 8:720–729.
7. Berman, J.W., M.P. Guida, J. Warren, J. Amat, and C.F. Brosnan. 1996. Localization of monocyte chemoattractant peptide-1 expression in the central nervous system in experimental autoimmune encephalomyelitis and trauma in the rat. *J. Immunol.* 156:3017–3023.
8. Valente, A.J., D.T. Graves, C.E. Vialle-Valentin, R. Delgado, and C.J. Schwartz. 1988. Purification of monocyte chemotactic factor secreted by nonhuman primate vascular cells in culture. *Biochemistry.* 27:4162–4168.
9. Carr, M.W., S.J. Roth, E. Luther, S.S. Rose, and T.A. Springer. 1994. Monocyte chemoattractant protein-1 acts as a T-lymphocyte chemoattractant. *Proc. Natl. Acad. Sci. USA.* 91:3652–3656.
10. Allavena, P., G. Bianchi, D. Zhou, J. Van Damme, P. Jilek, S. Sozzani, and A. Mantovani. 1994. Induction of natural killer cell migration by monocyte chemotactic protein-1, -2 and -3. *Eur. J. Immunol.* 24:3233–3236.
11. Jiang, Y., D.I. Beller, G. Frendl, and D.T. Graves. 1992. Monocyte chemoattractant protein-1 regulates adhesion molecule expression and cytokine production in human monocytes. *J. Immunol.* 148:2423–2428.
12. Kim, J.J., L.K. Nottingham, J.I. Sin, A. Tsai, L. Morrison, J. Oh, K. Dang, Y. Hu, K. Kazahaya, M. Bennett, et al. 1998. CD8 positive T cells influence antigen-specific immune responses through the expression of chemokines. *J. Clin. Invest.* 102:1112–1124.
13. Hogaboam, C.M., N.W. Lukacs, S.W. Chensue, R.M. Streiter, and S.L. Kunkel. 1998. Monocyte chemoattractant protein-1 synthesis by murine lung fibroblasts modulates $CD4^+$ T cell activation. *J. Immunol.* 160:4606–4614.
14. Taub, D.D., J.R. Ortaldo, S.M. Turcovski-Corrales, M.L. Key, D.L. Longo, and W.J. Murphy. 1996. β Chemokines costimulate lymphocyte cytolysis, proliferation, and lymphokine production. *J. Leukoc. Biol.* 59:81–89.
15. Gong, J.H., L.G. Ratkay, J.D. Waterfield, and I. Clark-Lewis. 1997. An antagonist of monocyte chemoattractant protein 1 (MCP-1) inhibits arthritis in the MRL-*lpr* mouse model. *J. Exp. Med.* 186:131–137.
16. Lloyd, C.M., A.W. Minto, M.E. Dorf, A. Proudfoot, T.N.C Wells, D.J. Salant, and J.C. Gutierrez-Ramos. 1997. RANTES and monocyte chemoattractant protein-1 (MCP-1) play an important role in the inflammatory phase of crescentic nephritis, but only MCP-1 is involved in crescent formation and interstitial fibrosis. *J. Exp. Med.* 185:1371–1380.
17. Smith, R.E., R.M. Streiter, K. Zhang, S.H. Phan, T.J. Standiford, N.W. Lukacs, and S.L. Kunkel. 1995. A role for C-C chemokines in fibrotic lung disease. *J. Leukoc. Biol.* 57:782–787.
18. Lukacs, N.W., R.M. Strieter, K. Warmington, P. Lincoln, S.W. Chensue, and S.L. Kunkel. 1997. Differential recruitment of leukocyte populations and alteration of airway hyperreactivity by C-C family chemokines in allergic airway inflammation. *J. Immunol.* 158:4398–4404.
19. Gonzalo, J.A., C.M. Lloyd, D. Wen, J.P. Albar, T.N. Wells, A. Proudfooot, A.C. Martinez, M. Dorf, T. Bjerke, A.J. Coyle, et al. 1998. The coordinated action of CC chemokines in the lung orchestrates allergic inflammation and airway hyperresponsiveness. *J. Exp. Med.* 188:157–167.
20. Lu, B., B.J. Rutledge, L. Gu, J. Fiorillo, N.W. Lukacs, S.L. Kunkel, R. North, C. Gerard, and B.J. Rollins. 1998. Abnormalities in monocyte recruitment and cytokine expression in monocyte chemoattractant protein 1–deficient mice. *J. Exp. Med.* 187:601–608.
21. Tesch, G.H., A. Schwarting, K. Kinoshita, H.Y. Lan, B.J. Rollins, and V. Rubin Kelley. 1999. MCP-1 promotes macrophage-mediated tubular injury, but not glomerular injury, in nephrotoxic serum nephritis. *J. Clin. Invest.* 103:73–80.
22. Rollins, B.J. 1997. Chemokines. *Blood.* 90:909–928.
23. Theofilopoulos, A.N., and F.J. Dixon. 1985. Murine models of systemic lupus erythematosus. *Adv. Immunol.* 37:269–390.
24. Wu, J., T. Zhou, J. He, and J.D. Mountz. 1993. Autoimmune disease in mice due to integration of an endogenous retrovirus in an apoptosis gene. *J. Exp. Med.* 178:461–468.
25. Schwarting, A., T. Wada, K. Kinoshita, G. Tesch, and V.R. Kelley. 1998. IFN-γ receptor signaling is essential for the initiation, acceleration, and destruction of autoimmune kidney disease in MRL-Fas^{lpr} mice. *J. Immunol.* 161:494–503.
26. Moore, K.J., T. Naito, C. Martin, and V.R. Kelley. 1996. Enhanced response of macrophages to CSF-1 in autoimmune mice. A gene transfer strategy. *J. Immunol.* 157:433–440.
27. Schwarting, A., K. Moore, T. Wada, G. Tesch, H.J. Yoon, and V. Rubin Kelley. 1998. IFN-γ limits macrophage ex-

pansion in MRL-*Fas*^{lpr} autoimmune interstitial nephritis: a negative regulatory pathway. *J. Immunol.* 160:4074–4081.
28. Lukacs, N.W., S.W. Chensue, R.E. Smith, R.M. Strieter, K. Warmington, C. Wilke, and S.L. Kunkel. 1994. Production of monocyte chemoattractant protein-1 and macrophage inflammatory protein-1 alpha by inflammatory granuloma fibroblasts. *Am. J. Pathol.* 144:711–718.
29. Natori, Y., M. Sekiguchi, Z. Ou, and Y. Natori. 1997. Gene expression of CC chemokines in experimental crescentic glomerulonephritis (CGN). *Clin. Exp. Immunol.* 109:143–148.
30. Jia, G.Q., J.A. Gonzalo, C. Lloyd, L. Kremer, L. Lu, A.C. Martinez, B.K. Wershil, and J.C. Gutierrez-Ramos. 1996. Distinct expression and function of the novel mouse chemokine monocyte-chemoattractant protein-5 in lung allergic inflammation. *J. Exp. Med.* 184:1939–1951.
31. O'Connell, P.J., A. Pacheco-Silva, P.W. Nickerson, R.A. Muggia, M. Bastos, V.R. Kelley, and T.B. Strom. 1993. Unmodified pancreatic islet allograft rejection results in the preferential expression of certain T cell activation transcripts. *J. Immunol.* 150:1093–1104.
32. Ezure, T., T. Ishiwata, G. Asano, S. Tanaka, and K. Yokomura. 1997. Production of macrophage colony-stimulating factor by murine liver in vivo. *Cytokine.* 9:53–58.
33. Russell, E.S. 1968. The Jackson Laboratory's Pedigreed Expansion Stocks. Lifespan and Aging Patterns. Biology of the Laboratory Mouse. E.A. Green, editor. Dover Publications, Inc., New York. 512 pp.
34. Bloom, R.D., S. Florquin, and V.R. Kelley. 1993. Colony stimulating factor-1 in the induction of lupus nephritis. *Kidney Int.* 43:1000–1009.
35. Naito, T., H. Yokoyama, K.J. Moore, G. Dranoff, R.C. Mulligan, and V.R. Kelley. 1996. Macrophage growth factors introduced into the kidney initiate renal injury. *Mol. Med.* 2:297–312.
36. Rovin, B.H., and L.T. Phan. 1998. Chemotactic factors and renal inflammation. *Am. J. Kidney Dis.* 31:1065–1084.
37. Watanabe-Fukunaga, R., C.I. Brannan, N.G. Copeland, N.A. Jenkins, and S. Nagata. 1992. Lymphoproliferation disorder in mice explained by defects in Fas antigen that mediates apoptosis. *Nature.* 356:314–317.
38. Tedla, N., H.W. Wang, H.P. McNeil, N. Di Girolamo, T. Hampartzoumian, D. Wakefield, and A. Lloyd. 1998. Regulation of T lymphocyte trafficking into lymph nodes during an immune response by the chemokines macrophage inflammatory protein (MIP)-1 alpha and MIP-1 beta. *J. Immunol.* 161: 5663–5672.
39. Moore, K.J., T. Wada, S.D. Barbee, and V.R. Kelley. 1998. Gene transfer of RANTES elicits autoimmune renal injury in MRL-Fas(lpr) mice. *Kidney Int.* 53:1631–1641.
40. Santoro, T.J., J.P. Portanova, and B.L. Kotzin. 1988. The contribution of L3T4$^+$ T cells to lymphoproliferation and autoantibody production in MRL-lpr/lpr mice. *J. Exp. Med.* 167:1713–1718.
41. Sobel, E.S., T. Katagiri, K. Katagiri, S.C. Morris, P.L. Cohen, and R.A. Eisenberg. 1991. An intrinsic B cell defect is required for the production of autoantibodies in the lpr model of murine systemic autoimmunity. *J. Exp. Med.* 173: 1441–1449.
42. Merino, R., M. Iwamoto, L. Fossati, and S. Izui. 1993. Polyclonal B cell activation arises from different mechanisms in lupus-prone (NZB × NZW)F1 and MRL/Mpj-lpr/lpr mice. *J. Immunol.* 151:6509–6516.
43. Izui, S., T. Berney, T. Shibata, and T. Fulpius. 1993. IgG3 cryoglobulins in autoimmune MRL-lpr/lpr mice: immunopathogenesis, therapeutic approaches and relevance to similar human diseases. *Ann. Rheum. Dis.* 52:S48–54 (Suppl.).
44. Haas, C., B. Ryffel, and M. Le Hir. 1997. IFN-γ is essential for the development of autoimmune glomerulonephritis in MRL/lpr mice. *J. Immunol.* 158:5484–5491.
45. Alexander, E.L., C.F. Moyer, G.S. Travlos, J.B. Roths and E.D. Murphy. 1985. Two histopathologic types of inflammatory vascular disease in MRL/Mp autoimmune mice. Model for human vasculitis in connective tissue disease. *Arthritis Rheum.* 28:1146–1155.
46. Bullard, D.C., B.D. King, M.J. Hicks, B. Dupont, A.L. Beaudet, and K.B. Elkon. 1997. Intercellular adhesion molecule-1 deficiency protects MRL/MpJ-Fas^{lpr} mice from early lethality. *J. Immunol.* 159:2058–2067.